Journal of Organometallic Chemistry, 187 (1980) 213—226
© Elsevier Sequoia S.A., Lausanne — Printed in The Netherlands

THE CRYSTAL STRUCTURE AND VARIABLE TEMPERATURE ^{119m}Sn MÖSSBAUER STUDY OF TRIMETHYLTIN GLYCINATE, A ONE-DIMENSIONAL, AMINO-BRIDGED POLYMER

B.Y.K. HO*, K.C. MOLLOY, J.J. ZUCKERMAN*

Department of Chemistry, University of Oklahoma, Norman, OK 73019 (U.S.A.)

F. REIDINGER and J.A. ZUBIETA

Department of Chemistry, State University of New York at Albany, Albany, NY 12222 (U.S.A.)

(Received June 4th, 1979)

Summary

The crystal structure of trimethyltin glycinate has been determined by Patterson and Fourier techniques to a final "R"-factor of 0.066 for 1103 unique reflections. The crystals are tetragonal with space group $P4_1$ with $a = b = 7.839(9)$ and $c = 14.659(11)$ Å, $Z = 4$, and are composed of stacks of linearly polymeric trimethyltin glycinate molecules bridged axially at tin through the amino nitrogen atoms of the amino acid. There is hydrogen bonding between carbonyl oxygen and amino group N—H moieties along the chains and between the chains to produce a perpendicular weave of one-dimensional polymer threads. The axial N---Sn—O connections make an angle approaching linearity, but the tin atom is distinctly displaced toward the oxygen to give non-planar SnC_3 units which are eclipsed in the ≡Sn—O—C(=O)—C—N---Sn≡ chain. This bridging rather than chelated amino acid configuration is only found in glycinatosilver(I) hemihydrate. Tin-119m Mössbauer resonance area data have been collected in the temperature range $77 \leqslant T \leqslant 185$ K, and a logarithmic plot of the normalized area vs. temperature is linear in this range and the slope of -1.15×10^{-2} K^{-1} yields values of the logarithmic temperature coefficient of the recoil-free fraction (which at 296 is less than a tenth of its value at 77 K). These data have been used to evaluate the isotropic mean-square amplitudes of vibration $\langle x_{iso}(T)^2 \rangle$ of the tin atom, normalized to the value at 296 K available from the crystallographic study, in the same temperature range. Isotropic-mean-square values of the vibrational amplitude increase from 1.78×10^{-2} at 77 to 2.63×10^{-2} at 185 and 3.5×10^{-2} at 296 K. From the doublet line asymmetry data, and assuming that the electric field

* Present address: Ferro Corporation, P.O. Box 46349, Bedford, OH 44146.

gradient tensor, V_{zz}, is positive in sign and lies along the polymer axis (oblate field about the cylindrical axis), it is concluded that the tin atom vibrates with greater amplitude normal to the propagating axis ($\langle x_\perp^2 \rangle = 1.93 \times 10^{-2}$ at 77 and 3.11×10^{-2} Å^2 at 185 K) than along it ($\langle x_\parallel^2 \rangle = 1.48 \times 10^{-2}$ at 77 and 1.67×10^{-2} Å^2 at 185 K). The temperature coefficient of the motion normal to the axis is also greater over the range examined. The difference in the mean-square amplitudes perpendicular and parallel to the axis are 2.96×10^{-2} from the Mössbauer treatment and 4.24×10^{-2} Å^2 from the X-ray anisotropic thermal ellipsoids at 296 K.

Triorganotin compounds are important biocides [1,2], and the study of their amino acid derivatives, which are themselves biocidal [3], can help to elucidate their mode of action. The structures of these species, of which trimethyltin glycinate is the simplest example, are of interest from two chemical points of view. Carboxylate group bridging between trigonal planar trimethyltin moieties is now well-established in the acetates [4] and would compete with amino-nitrogen bridging in the amino acid derivatives. However, metal ions are generally chelated by amino acids [5], while the triorganotin moieties bind preferentially [4] in an axially-most-electronegative fashion, a situation which would lead to an associated polymer structure instead.

We have used spectroscopic evidence to show that trimethyltin glycinate is a one-dimensional polymer with bridging amino groups. Lowered amino group N—H infrared frequencies and enhanced intensities indicate that nitrogen is involved in coordination. The tin-119m Mössbauer quadrupole splitting (*QS*) values and its ratio to the isomer shift (*IS*) establish that the tin atom is in a higher than four-coordinated environment. Pronounced line intensity asymmetry in the doublet spectrum, and the observation of the resonance at ambient temperature confirms a polymeric structure *. High carboxylate stretching frequencies in the infrared rule out carbonyl oxygen coordination to tin, and infrared and Raman data in the tin—carbon stretching region rule out a precisely planar SnC_3 skeleton [9] **.

Trimethyltin glycinate, m.p. 163—164°C decomp., is formed in 80% yield by the azeotropic distillation of water from trimethyltin hydroxide and glycine in benzene with *N*,*N*-dimethylformamide as a catalyst:

$$(CH_3)_3SnOH + HOCCH_2NH_2 \rightarrow (CH_3)_3SnOCCH_2NH_2 + H_2O \qquad (1)$$

The physical properties of the products are listed in Table 1.

This paper reports the full details of the X-ray crystallographic structure of trimethyltin glycinate, and discusses variable temperature tin-119m Mössbauer and low energy, lattice mode Raman data in terms of the lattice dynamics of the structure.

---

* The observations of ambient-temperature tin-119m Mössbauer spectra for certain molecular solids [6] does not affect our conclusion which is based upon close analogy with other tin(II) [7] and tin(IV) [8] amines.

** The results of this study have been communicated in a preliminary report [10].

TABLE 1

THE PHYSICAL PROPERTIES OF TRIMETHYLTIN GLYCINATE [a]

Infrared frequencies	
Amino Group	3311, 3244, 3224, 3199, 3154 cm^{-1}
Carboxylate Group	ν_{asym} 1630; ν_{sym} 1398 cm^{-1}
Me_3Sn Group	ν_{asym} 545; ν_{sym} 507 cm^{-1}
	Raman 542, 507 cm^{-1}
Mössbauer data at 77 K	*IS* = 1.18 ± 0.02 mm/s
	QS = 3.36 ± 0.04 mm/s

[a] Ref. 9.

Experimental section and structure refinement

Single crystals of trimethyltin glycinate used for X-ray study were grown by sublimation at a pressure of 90 Torr using a pointed cold finger kept at —78°C with an oil bath temperature of 140—150°C.

Tetragonal crystals of the compound were mounted in nitrogen-filled Lindemann glass capillary tubes. Approximate unit cell dimensions and the space group were determined from preliminary Weissenberg and precession photographs using nickel-filtered Cu-K_α radiation (λ 1.5418 Å). The details of the crystal parameters and data measurement and reduction are given in Table 2.

TABLE 2

EXPERIMENTAL DETAILS OF THE X-RAY DIFFRACTION STUDY OF TRIMETHYLTIN GLYCINATE

	(A) Crystal parameters [a] at 23°C
a = 7.839(9) Å	Space Group $P4_1$
b = 7.839(9) Å	Z = 4
c = 14.659(11) Å	ρ(calcd) = 1.75 g/cm^3
V = 900.79 $Å^3$	ρ(found) [b] = 1.73 g/cm^3
	(B) Measurement of intensity data
Instrument:	Siemens' AED quarter-circle diffractometer
Radiation:	Cu-K_α(λ = 1.5418 Å)
Attenuator:	used for counts > 100 000/s
Scan mode:	Coupled θ(crystal) — 2θ(counter).
Scan rate:	Variable, within limits of 0.25 to 2.0°/min.
Scan range:	$2.0 < 2\theta < 140.0°$
Scan length:	from $2\theta(K_{\alpha_1})$ — 0.95° to $2\theta(K_{\alpha_2})$ + 0.95°
Background measurements:	Stationary crystal — stationary counter, at each end of 2θ scan range for a time equal to the peak intensity measurement.
Standards:	Three reflections measured every 32 data.
No. of reflections collected:	1103
	(C) Reduction of intensity data [c]
Data corrected for background, attenuators, Lorentz polarization, and absorption in the usual fashion [d]	
Absorption coefficient:	229.1 cm^{-1}
Averaging:	Over two equivalent forms, using a local program.
Observed data:	824 unique reflections for which $I_{obs} > 2.58\sigma(I_{obs})$.

[a] From a least-squares fit to the setting angles of 12 reflections. [b] Pycnometer. [c] Programs for the UNIVAC 1100 computer used in this work are described in ref. 26. [d] Data reduction was performed as described in ref. 27. Atomic scattering factors were taken from ref. 28. The range of the transmission factors was 0.45—0.83 for a crystal of 0.15 X 0.30 X 0.15 mm.

TABLE 3

FINAL POSITIONAL AND THERMAL PARAMETERS FOR TRIMETHYLTIN GLYCINATE [a]

Atom	x	y	z	U or U_{11} [b]	U_{22}	U_{33}	U_{12}	U_{13}	U_{23}
Sn	0.4899(2)	0.0367(1)	0.2500	3.82(9)	1.10(6)	5.71(8)	−0.12(8)	−0.11(7)	1.30(12)
O(1)	0.4073(22)	0.3044(17)	0.2646(13)	4.18(38)					
O(2)	0.6503(22)	0.4026(23)	0.1955(12)	4.75(42)					
N(1)	0.5678(26)	0.7341(20)	0.2644(17)	4.04(44)					
C(1)	0.7128(41)	0.0678(39)	0.3325(22)	6.29(77)					
C(2)	0.5043(38)	0.0227(33)	0.1028(20)	5.86(70)					
C(3)	0.2599(43)	−0.0216(42)	0.3174(23)	6.91(87)					
C(4)	0.4314(27)	0.6071(24)	0.2361(16)	3.40(49)					
C(5)	0.5090(30)	0.4254(27)	0.2298(15)	3.78(54)					

[a] Estimated standard deviations are given in parenthesis. [b] $U_{ij} \times 10^2$. The vibrational coefficients refer to the expression: $T = \exp[-2\pi^2(U_{11}h^2a^{*2} + U_{33}l^2c^{*2} + 2U_{12}hka^*b^* + 2U_{13}hla^*c^* + 2U_{33}klb^*c^*]$.

TABLE 4

SELECTED BOND LENGTHS AND ANGLES FOR TRIMETHYLTIN GLYCINATE
(estimated standard deviations in parentheses)

Sn—O(1)	2.21(1)	O(1)—C(5)	1.34(3)
Sn′—N(1) [a]	2.46(2)	O(2)—C(5)	1.23(3)
Sn—C(1)	2.14(3)	C(4)—C(5)	1.55(3)
Sn—C(2)	2.16(3)	N—C(4)	1.51(3)
Sn—C(3)	2.11(3)		
N—Sn—O(1)	169.2(6)	Sn—O(1)—C(5)	117.5(14)
O(1)—Sn—C(1)	94.4(10)	Sn—N—C(4)	116.2(13)
O(1)—Sn—C(2)	99.2(9)	O(1)—C(5)—O(2)	126.1(21)
O(1)—Sn—C(3)	84.8(10)	O(1)—C(5)—C(4)	112.7(18)
N—Sn—C(1)	81.9(10)	O(2)—C(5)—C(4)	121.2(20)
N—Sn—C(2)	91.4(9)	C(5)—C(4)—N	110.3(17)
N—Sn—C(3)	87.9(10)		
C(1)—Sn—C(2)	121.8(11)		
C(1)—Sn—C(3)	117.3(12)		
C(2)—Sn—C(3)	120.1(12)		

[a] This is a tin atom such that if Sn is at coordinates x, y, z, then Sn′ is at coordinates $x, y + 1, z$.

The x- and y-coordinates for the tin positions were determined from the Patterson map; the z-coordinate was set at 0.2500 ($R_1 = 0.18$). Subsequent Fourier maps disclosed the positions of all non-hydrogen atoms. Anomalous dispersion corrections were introduced for tin, and anisotropic and isotropic temperature factors refined for the tin and all non-hydrogen, light atoms, respectively. Refinement converged to $R = 0.069$ where $R = \Sigma||F_o| - |F_c||/\Sigma|F_o|$. The error as an observation of unit weight, $[\Sigma w\Delta^2/(N_o - N_v)]^{1/2}$, was 2.05 *.

The final difference Fourier displayed considerable residual electron density in the vicinity of the tin atom and several regions of electron density of 0.8 to 1.8 $e/Å^3$. Although some of these peaks corresponded to potential hydrogen atom positions, the generally poor quality of the map precluded a systematic search for hydrogen atoms.

Atomic positional and thermal parameters, along with their standard deviations, are presented in Table 3. Table 4 summarizes relevant bond distances and angles. The coordination geometry about the tin is depicted in Fig. 1.

Mössbauer spectra were recorded on a Ranger Engineering constant acceleration spectrometer equipped with an NaI scintillation counter and using $Ca^{119m}SnO_3$ (New England Nuclear Corp.) as both source and standard reference material for zero velocity. Velocity calibration was based on both β-tin and natural iron. Data were fitted to Lorentzian curves by standard non-linear, least squares techniques, using an adaptation of the NLLSQ program developed by Dr. E.L. Enwall of this Department. The Ranger Engineering variable temperature liquid nitrogen dewar and controller used in these studies is regulated by a variable bridge, silicon-controlled-rectifier circuit and is accurate to within ±1 K.

Raman data were taken on a Spex Ramalog 5 laser Raman spectrometer using a 514.5 nm source.

* See NAPS document no. 03548 for 9 pages of supplementary material. Order from NAPS c/o Microfiche Publications, P.O. Box 3513, Grand Central Station, New York, N.Y. 10017. Remit in advance, in U.S. funds only $ 5.00 for photocopies or $ 3.00 for microfiche. Outside the U.S. and Canada add postage of $ 3.00 for photocopy and $ 1.00 for microfiche.

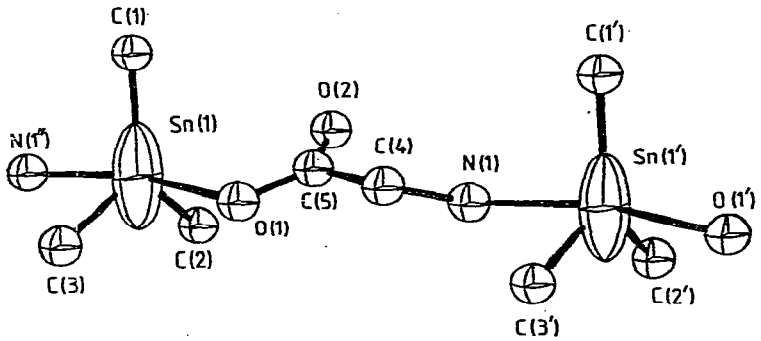

Fig. 1. The asymmetric unit of trimethyltin glycinate. Primed atoms are related to those in the asymmetric unit by $x, y + 1, z$; double primed atoms are related by $x, y - 1, z$.

Discussion

The structure

The structural analysis confirms the amino nitrogen coordination to tin and the distorted trigonal bipyramidal geometry with the more electronegative substituents occupying the apical positions. The SnC_3 skeleton is distinctly nonplanar and there is C_{3v} local symmetry with the tin atom displaced toward the carboxylate oxygen 0.11 Å from the mean plane of the methyl carbons.

The stereochemistry of the polymer is determined by the axially-most-electronegative arrangement at tin. The five-membered chelate rings which are characteristic of the complexes amino acids make with metals are thus precluded in the linear arrangement of the ligand oxygen and nitrogen atoms in the apical positions of the trigonal bipyramid about tin. The result is a one-dimensional, infinite chain, an arrangement common in triorganotin chemistry [4], but in amino acid coordination found in only glycinatosilver(I) hemihydrate [11], in which the preferred digonal coordination at silver (I) predominates to determine the stereochemistry [5].

The coordination through the amino nitrogen atom is unusual since the affinity of tin for oxygen coordination is believed to be greater. In addition, the alternative carboxylate bridging would give rise to short, strong, three-atom Sn—O—C=O—Sn bridges which should bring tin atoms in adjacent molecules to within ca. 7 Å [4] (measured along the bond vectors), rather than the longer and presumably weaker four-atom Sn—O—C(=O)—C—N—Sn bridges found here at ca. 9 Å (or 7.839 Å for the direct, across space, tin—tin distance within each chain).

The tin—carboxylate carbonyl oxygen contact distance across space is only 3.23(2) Å (Sn—O(2)), and the C(5)—O(1) bond seems to be rotated to bring the oxygen into juxtaposition with the tin atom. Comparable tin(IV)—oxygen coordination distances are in the range 2.11 to 2.49 Å for six-coordinated, chelated structures [4]. Tricyclohexyltin acetate is an analogous case. Its monomeric structure is described as a flattened tetrahedron with wide tin—carbon angles in which the carboxylate oxygen atom lies 2.95 Å from the tin in a stereochemically significant position [12]. The distance is not only larger in our glycinate, but the tin—carbon angles are almost exactly 120°, precluding the additional stabiliza-

tion of the lattice which would come about through intramolecular chelation with the carboxylate oxygen. Additional stabilization does come about, however, through hydrogen bonding between this carbonyl oxygen (O(2)) and the amino group N—H which lies 2.86(2) Å distant along the chain.

The axial nitrogen—tin—oxygen angle is 169.2(6)°, and the trimethyltin groups are eclipsed as in the recently solved structure of trimethyltin chloride, another one-dimensional associated polymer with a nearly linear X—Sn—X backbone [13], and unlike the situation found with the SnC_3 moieties in the trimethyltin methoxide [14] or cyclohexanone oxime [15] polymers which contain O—Sn—O backbones.

Adjacent sheets of linear polymer chains are related to one another in a perpendicular fashion to produce the cross-wise weave which makes up a lattice consistent with the four-fold screw axis demanded by the space group. The unit cell contents are shown in Fig. 2. The lattice is stabilized by hydrogen bonding between an amino group N—H and a symmetry related carbonyl oxygen (O(2)) 2.74(3) Å distant in an adjacent chain. The crystal propagates along the *c*-axis, and not along the propagation axes of the polymer chains which lie along *a* and *b*. Hence, we are forced to conclude that the intermolecular, interchain hydrogen bonding makes a more important contribution to the lattice energy than the coordinate covalent bonding of nitrogen to tin.

Variable temperature Mössbauer study

The Mössbauer recoil-free fraction, *f*, reflects the binding strength of the lattice since it is a function of the mean-square-displacement, $\langle x^2 \rangle$ of the tin atom from its equilibrium position:

$$f = \exp\left[-\frac{\langle x^2 \rangle}{\lambda 2}\right] \tag{2}$$

where λ is the wavelength of the Mössbauer γ-ray. For thin absorbers, using the Debye model, the recoil-free fraction is linearly related to the area under the resonance, A_T, and its temperature dependence is given by:

$$A_T \{f = \exp\left[-\frac{6E_R T}{k\theta_D^2}\right] \text{ for } T \geqslant \frac{\theta_D}{2} \tag{3}$$

where E_R is the Mössbauer recoil energy, and θ_D is the Debye temperature of the solid. Thus in the high temperature limit, plots of ln A_T vs. temperature should be linear. It is found that the more tightly bound the tin atoms are in a lattice, the slower will be the decrease of *f*, and hence A_T, as the temperature is raised. Compounds of known structure consisting of non-interacting monomeric molecules exhibit slopes of ca. -1.8×10^{-2} K^{-1}, no matter what the coordination number at tin. Weak intermolecular interactions such as hydrogen bonding reduce this value to ca. -1.7×10^{-2} K^{-1} while a more complex system of hydrogen bonds reduces it further to ca. -1.3×10^{-2} K^{-1}. Strongly hydrogen bonded lattices and solids in which one-, two- and three-dimensional association is present exhibit slopes of ca. -0.9×10^{-2} K^{-1}. Tin(II) oxide gives the lowest value, -0.23×10^{-2} K^{-1} [16,17].

The plot of ln (A_T/A_{77}) (normalized to the area under the resonance curves at 77 K) vs. temperature for trimethyltin glycinate between 77 and 185 K which

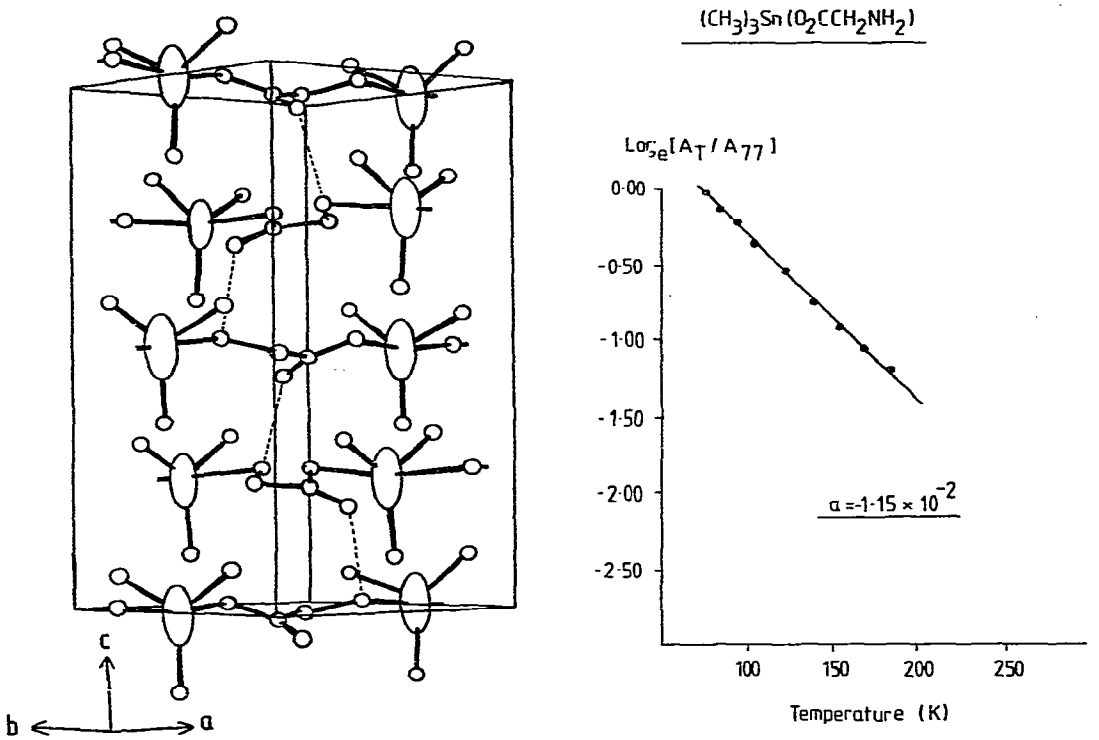

Fig. 2. The unit cell of trimethyltin glycinate. Alternate polymer chains are at right angles to each other, producing a cross-wise weave. Dashed lines intermolecular hydrogen bonding.

Fig. 3. The plot of ln A (normalized to the area under the resonance curve at 77 K) vs. temperature in K. The slope, α, is -1.15×10^{-2} K^{-1}.

is shown in Fig. 3 has a slope of -1.15×10^{-2} K^{-1} (intercept at $T = 0$, 0.882, correlation coefficient 0.999, number of points 9). This value corresponds to a recoil-free fraction, f, which decays rapidly from 7.35×10^{-2} at 77 to 2.11×10^{-2} at 185 and 5.9×10^{-3} at 296 K, the temperature at which the X-ray structural determination was carried out, and can be compared with others derived for known, one-dimensional, associated polymers such as trimethyltin cyclohexanone oxime $(CH_3)_3SnONC_6H_{10}$ [15], which exhibits a slope of -0.97×10^{-2} K^{-1} [16,17] *. It must be noted that in this case the bridging group is a single

* The reporting of the temperature dependence of Mössbauer resonance areas is in a confused state. The slope data for trimethyltin fluoride, for example, listed in ref. 18 as $d\log_{10}A/dT = 6.13 \times 10^{-3}$ K^{-1}, or $d\ln A/dT = 1.41 \times 10^{-2}$ K^{-1} are quoted by Herber et al. [29] as $\ln f = -1.75 \times 10^{2} - 5.95/T$, or $d\ln f/dT = -1.75 \times 10^{+2}$ K. The correct value should of course be -1.75×10^{-2} K^{-1} as quoted by Hazony and Herber later [30]. The corresponding slope for trimethyltin azide, whose one-dimensional, polymeric structure associated through the α-nitrogen atom we have recently solved [31] is said to be identical [32] but is quoted by Silverstri et al. [33] as $d\ln A/dT = 6.13 \times 10^{-2}$ K^{-1} rather than $d\log_{10}A/dT = 6.13 \times 10^{-3}$ K^{-1}, or the correct value for the fluoride which is $d\ln A/dT = -1.75 \times 10^{-2}$ K^{-1}. The slopes for these linear polymers, both associated through one-atom bridges, are somewhat too high according to the systematics described in ref. 17, and these measurements should be repeated. Such plots should employ slopes normalized to the areas at 77 K to facilitate comparison, and regression analysis data listed. Using the numerical data listed for trimethyltin isocyanate in ref. 34 we obtain $d\ln A/dT = -2.11 \times 10^{-2}$ K^{-1}, and not 4.47×10^{-2} K^{-1} as calculated in the paper and quoted by Silverstri et al. [33]. In addition, the tabulated data refer to four temperatures in the range 78 K $< T <$ 202 K while six points (120 K $< T <$ 220 K) are plotted.

atom, Sn—O—Sn, and the distance along the bonds from tin to tin is 4.67 Å [15]. In trimethyltin glycinate, by contrast, the tin atoms are separated by four

atoms, Sn—O—C—C—N—Sn, and nearly 9 Å. The tightness of the lattice in this case must arise less from the polymer chain interactions through bridging nitrogen than from the C=O—H—N hydrogen bonds formed in and between the chains, since the former is subject to a large "concertina-effect" through the four bridging atoms.

The $\langle x^2_{iso} \rangle$ values can be calculated at all temperatures given the temperature dependence and one value of $\langle x^2_{iso} \rangle$. The former is derived from the derivative of eq. 2 with respect to temperature, i.e., $d\langle x^2_{iso} \rangle / dT = -\chi(d\ln A/dT)$, and the latter is derived from X-ray data. The values of $\langle x^2_{iso} \rangle$ of the tin atom in our structure range from 1.78×10^{-2} at 77 to 2.63×10^{-2} at 185 and 3.5×10^{-2} Å^2 at 296 K (extrapolated).

The effective vibrating mass model

A model has been developed by Herber which applies data from the variation of the recoil-free fraction with temperature and the low energy (<200 cm^{-1}) lattice mode absorptions in the Raman spectrum to obtain the mass of the vibrating unit in the solid [19]. The treatment is based upon a Debye solid, and allows the molecularity of the vibrating unit to be calculated from:

$$M_{eff} = -\frac{3E_\gamma{}^2 k}{(hc)^2 \omega_L{}^2}\left(\frac{dT}{d\ln A}\right) \qquad (4)$$

where $-(d\ln A/dt) = 1.15 \times 10^{-2}$ K^{-1}, the slope of the plot of the normalized area vs. temperature and E_γ is the energy of the Mössbauer γ-ray. The low energy Raman spectrum which should contain the frequency ω is shown in Fig. 4 for trimethyltin glycinate. There are no data in the literature of which we are aware that could otherwise serve as a guide to the assignment of the four Raman-active bands found below 50 cm^{-1}. The infrared spectrum of glycine in a Nujol mull contains no bands below 132 cm^{-1} at 298 K, but bands at just above 70 and just below 80 cm^{-1} can be discerned at 113 K [20]. Table 5 lists the correlation between the ω frequencies and the M_{eff} values. The molecular weight of the trimethyltin glycinate monomer is calculated to be 238. Frequencies above the 46 cm^{-1} band cannot, therefore, correspond to the unique intermolecular intra-unit cell vibration sought in this treatment. The bands observed correspond to the motion of a dimer, tetramer or heptamer. No band corresponding to the monomer (238 corresponds to a lattice frequency of 61 cm^{-1}) is observed. There are four molecules in the unit cell, and the frequency observed at 46 cm^{-1} can be assigned to the vibration of two molecular units in one pair of chains against two adjacent molecular units in a second pair of chains. The results are thus consistent with the polymeric chain structure, and especially the hydrogen bonding of C—O—H—N groups in adjacent chains giving rise to linking of groups in the structure.

Temperature variation of the Goldanskii—Karyagin effect

The anisotropy of the Mössbauer recoil-free fraction, commonly called the Goldanskii-Karyagin effect [21,22], and observed as an asymmetry in the

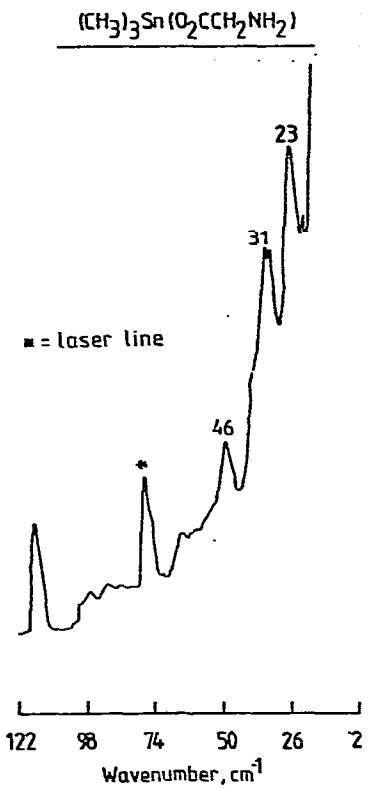

Fig. 4. The Raman spectrum of trimethyltin glycinate below 125 cm^{-1}.

relative intensities of the two lines in a doublet spectrum, can also yield information about the lattice dynamics of solids, especially if X-ray diffraction data on the structure are also available. The application to trimethyltin glycinate is ideal since a welldefined z-axis propagating along the —N—Sn—O— chain [<N—Sn—O=1.69.2(6)°] in which the amplitude of vibration is expected to be smallest, is available, the two components of the Mössbauer resonance doublet are easily resolved and the areas measured, and large resonance effects are observed, even for thin absorbers. It is possible to obtain information about the mean-square amplitudes of vibration parallel ($\langle x_{\parallel}^2 \rangle$) and normal ($\langle x_{\perp}^2 \rangle$) to the z-axis chain from the measurement of f-values for the two resonance lines.

TABLE 5

LOW ENERGY LATTICE MODE RAMAN FREQUENCIES AND M_{eff} VALUES IN THE EFFECTIVE VIBRATING MASS MODEL

$\omega(cm^{-1})$	M_{eff}	Molecular weight multiple
23	1684	7; 1666
31	927	4; 952
38(sh)	617	—
46	421	2; 476

By analogy with the treatment of $(CH_3)_3SnCN$ [23], we will assume that the electrostatic field has an oblate shape about the axis of cylindrical symmetry (N—Sn—O), and hence that V_{zz}, the principle component of the electric field gradient tensor, is positive. An oblate field acting on a ^{119}Sn nucleus moves the 3/2 level to lower energy, and R (the ratio of the area under the more positive velocity component of the quadrupole split spectrum to the area of the more negative component) = $A_+/A_- = A_\sigma/A_\pi$. Thus for trimethyltin glycinate, like the analogous cyanide [23], the $\pm\frac{1}{2}$ level of the excited, isomeric state is at a higher energy and the $\pm\frac{3}{2}$ state at a lower one. Consequently, the doublet component at higher velocities corresponds to the $\Delta m = 0$(sigma) transition while the other component corresponds to the $\Delta m = \pm 1$(pi) transition. In the trigonal bipyramidal glycinate structure the bulk of the electron density should lie in the $SnC_3(x, y)$ plane, and hence an oblate field and a positive V_{zz} are reasonable.

The mean square amplitude of vibration parallel and normal to V_{zz} can be expressed as:

$$A\left\{\ln f = -\frac{1}{3\lambda_2}\left[2\langle x_\parallel^2\rangle + \langle x_\perp^2\rangle\right]\right. \tag{5}$$

where λ is the wavelength of the Mössbauer γ ray, or in terms of an asymmetry factor, ϵ, where:

$$\epsilon = [\langle x_\parallel^2\rangle - \langle x_\perp^2\rangle]/\lambda^2$$

and hence,

$$\langle x_\parallel^2\rangle = \lambda^2\left(\frac{2\epsilon}{3} - \ln f\right) \tag{7}$$

$$\langle x_\perp^2\rangle = -\lambda^2\left(\frac{\epsilon}{3} + \ln f\right) \tag{8}$$

Of the four variables in these two equations, ϵ, f, $\langle x_\parallel^2\rangle$ and $\langle x_\perp^2\rangle$, ϵ can be calculated from the temperature-dependence of A_π/A_σ, and f from the temperature-dependence of the total area under the resonance and one value of f. The latter value may be derived indirectly from the X-ray thermal data at 293 K and eq. 2.

The temperature dependence of the ratio A_+/A_- is linear (slope 1.66×10^{-3} K^{-1}, intercept 1.037, correlation coefficient 0.994, number of points 9) as shown in Fig. 5 over the range 77 to 185 K.

Using the temperature dependence of the total area, the temperature dependence of $\langle x_\parallel^2\rangle$ and $\langle x_\perp^2\rangle$ can be plotted, as in Fig. 6. It is seen that the anisotropy parameter, ϵ, is always negative in the range measured, that is, $\langle x_\parallel^2\rangle < \langle x_\perp^2\rangle$ for any temperature in that range. The area ratios, when extrapolated to absolute zero, based upon the data observed experimentally in the range 77 to 185 K, give 1.037 which corresponds to virtually isotropic motion of the tin atom at this temperature. The equations of the two plots are:

$$\frac{d\langle x_\parallel^2\rangle}{dT} = 1.816 \times 10^{-5}\, T + 1.353 \times 10^{-2} \tag{9}$$

(with the regression analysis data: correlation coefficient 0.904, number of

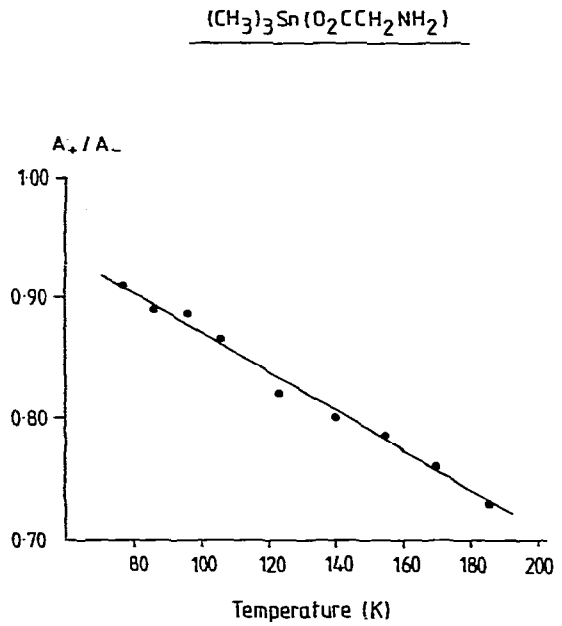

Fig. 5. The temperature-dependence of the ratio of the area of the higher velocity (A_+) resonance line to that lower (A_-) over the 77 to 185 K range.

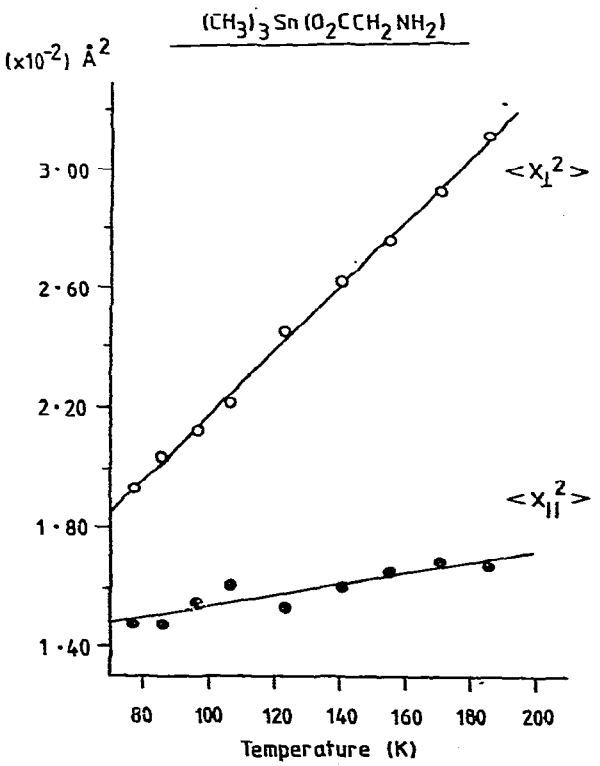

Fig. 6. The temperature-dependence of $\langle x_{\parallel}^2 \rangle$ and $\langle x_{\perp}^2 \rangle$ in Å between 77 and 185 K.

points 9), and

$$\frac{d\langle x_{\perp}^2\rangle}{dT} = 1.088 \times 10^{-4}\, T + 1.088 \times 10^{-2} \qquad (10)$$

(correlation coefficient 0.998, number of points 9). The mean-square amplitudes of vibration, $\langle x_{\parallel}^2\rangle$ and $\langle x_{\perp}^2\rangle$, are 1.48×10^{-2} and 1.93×10^{-2} Å, respectively, at 77 K and 1.67×10^{-2} and 3.11×10^{-2} Å at 185 K.

The anisotropic thermal ellipsoids from the X-ray data at 23°C give root-mean-square amplitudes of vibration of the tin atom as 6.01 and 3.95×10^{-2} Å along the $x_{\perp}^2$ direction, and 7.43×10^{-3} Å along the $x_{\parallel}^2$ direction. From these data the difference in the mean-squared amplitudes perpendicular and parallel to the z-axis of polymer propagation is 4.24×10^{-2} Å^2. From these data the same value at 296 K from the Mössbauer treatment is 2.96×10^{-2} Å^2, which is in rough qualitative agreement with there being greater anisotropy appearing from the X-ray treatment between $\langle x_{\parallel}^2\rangle$ and $\langle x_{\perp}^2\rangle$ at ambient temperatures.

Part of the discrepancy lies in the fact that the bonding axes, which constrain the motion of the tin atom to the greatest extent, do not exactly coincide with the x-, y- and z-axes (the principal axes) of the anisotropic thermal ellipsoids, nor is the molecular symmetry C_{3v} as assumed in this treatment. Hence, since $x_{\perp}$ is not precisely disposed along the SnC_3 bonds, the values for this parameter appear larger from the X-ray data, i.e., the tin atom appears to be more free to move in the $x_{\perp}$ direction from the anisotropic thermal ellipsoids seen in Fig. 2 than is in fact the case.

Conclusions

Trialkyltins seem to have little or no affinity for mono- or di-thiols, and they do not bind to many biologically important macromolecules such as cytochrome c, hemoglobin, myoglobin, chymotripsin, glycogen, etc. Yet trialkyltins are extremely biocidal, and severely inhibit mitochondrial function. The hypothesis has been advanced that the trialkyltin binds to mitochondria by pentacoordination between nitrogen atoms of two histidine sites [24]. In this regard the structure of trimethyltin glycinate is important in establishing that the binding can involve the nitrogen atom of the amino acid, and in contributing to an understanding of the nature of the effect of the axial-connection on the configuration of the amino acid. The disruption of mitochondria and the disorganization of muscle fibres brought about by the trialkyltin treatment have recently been observed under the electron microscope [25]. These effects may be related to the axial-binding seen in the glycinate structure.

Acknowledgement

Our work is supported by the Office of Naval Research and the National Science Foundation under Grant CHE-78-26584. We thank M & T Chemicals, Inc. for the donation of organotin starting materials, Mr. G.A. Blasi for help with the computations, Professor R.E. Frech for help with recording the Raman spectra, and Professors H. Chessin of the State University of New York at Albany and D. van der Helm of the University of Oklahoma for helpful discussions.

References

1 J.J. Zuckerman, R.P. Reisdorf, H.V. Ellis, III and R.R. Wilkinson, Organotins in Biology and the Environment, in J.M. Bellama and F.E. Brinckman (Eds.), Chemical Problems in the Environment: Occurrence and Fate of the Organoelements, Brinckman, ACS Symposium Series, No. 82, American Chemical Society, Washington, D.C., 1978, p. 388.
2 J.J. Zuckerman (Ed.), Organotin compounds: New Chemistry and Applications, Advances in Chemistry Series, No. 157, American Chemical Society, Washington, D.C. 1976.
3 (a) D.A. Kochkin, S.G. Verenkina and I.B. Chekmareva, Dokl. Akad. Nauk SSSR, 139 (1961) 1375; (b) D.A. Kochkin and M.G. Golysheva, Tr. Vses. Nauch.-Issled. Vitamin. Inst., 8 (1961) 82; Chem. Abstr., 57 (1962) 3850d; (c) D.A. Kochkin and S.G. Verenikina, Tr. Vses. Nauch.-Issled. Vitamin. Inst., 8 (1961) 39; Chem. Abstr., 58 (1963) 6851; (d) M.J. Koopmans, Dutch Patent 96, 805 (1961); Chem. Abstr., 55 (1961) 27756f.
4 J.A. Zubieta and J.J. Zuckerman, Prog. Inorg. Chem., 24 (1978) 251.
5 R. Osterberg, Coord. Chem. Rev., 12 (1974) 309.
6 G.M. Bancroft, K.D. Butler and T.K. Sham, J. Chem. Soc., Dalton Trans., (1975) 1483.
7 P.J. Corvan and J.J. Zuckerman, Inorg. Chem. Acta, 34 (1979) L255.
8 M.E. Bishop and J.J. Zuckerman, Inorg. Chem., 16 (1977) 1749.
9 B.Y.K. Ho and J.J. Zuckerman, Inorg. Chem., 12 (1973) 1552.
10 B.Y.K. Ho, J.A. Zubieta and J.J. Zuckerman, J. Chem. Soc., Chem. Communs., (1975) 88.
11 C.B. Acland and H.C. Freeman, J. Chem. Soc., Chem. Commun., (1971) 1016.
12 N.W. Alcock and R.E. Timms, J. Chem. Soc., A, (1968) 1876.
13 M.B. Hossain, J.L. Lefferts, K.C. Molloy, D. van der Helm and J.J. Zuckerman, Inorg. Chim. Acta, 36 (1979) L409.
14 A.M. Domingos and G.M. Sheldrick, Acta Cryst. B, 30 (1974) 519.
15 P.F.R. Ewings, P.G. Harrison, T.J. King, R.C. Phillips and J.A. Richards, J. Chem. Soc., Dalton Trans., (1975) 1950.
16 P.G. Harrison, in ref. 2, p. 258.
17 P.G. Harrison, R.C. Phillips and E.W. Thornton, J. Chem. Soc., Chem. Commun., (1977) 603.
18 R.H. Herber and S. Chandra, J. Chem. Phys., 54 (1971) 1847.
19 R.H. Herber and M.F. Leahy, in ref. 2, p. 155.
20 W.R. Fearheller and J.T. Miller, Jr., Appl. Spectrosc., 25 (1971) 275.
21 N.N. Greenwood and T.C. Gibb, Mössbauer Spectroscopy, Chapman and Hall, London, 1971.
22 T.C. Gibb, Principles of Mössbauer Spectroscopy, Chapman and Hall, London 1976.
23 R.H. Herber, S. Chandra and Y. Hazony, J. Chem. Phys., 53 (1970) 3330.
24 W.N. Aldridge, in ref. 2, p. 186.
25 L.P. Tan and M.L. Ng, J. Neurochem., 29 (1977) 689.
26 J.M. Stewart, G.J. Kruger, H.L. Ammon, D. Dickinson and S.R. Hall, Techn. report TR-192, University of Maryland, June, 1972.
27 J.R. Dilworth, J. Hyde, P. Lyford, P. Vells, K. Venkatasubramanian and J.A. Zbubieta, Inorg. Chem., in press.
28 D.T. Cromer and J.T. Waber, Acta Cryst., 18 (1965) 104.
29 R.H. Herber, J. Fischer and Y. Hazony, J. Chem. Phys., 58 (1973) 5185.
30 Y. Hazony and R.H. Herber in I.J. Gruverman and C.W. Seidel (Eds.), Mössbauer Effect Methodology, Plenum Press, New York, 1973, Vol. 8, p. 107.
31 D. Cunningham, K.C. Molloy, D. van der Helm and J.J. Zuckerman, submitted.
32 R.H. Herber and H.S. Cheng, Inorg. Chem., 9 (1970) 1686.
33 A. Silverstri, E. Rivarola and R. Barbieri, Inorg. Chim. Acta, 23 (1977) 149.
34 K.L. Leung and R.H. Herber, Inorg. Chem., 10 (1971) 1020.